Clin Orthop Relat Res (2018) 476:2076-2090
DOI 10.1097/CORR.0000000000000395

Clinical Orthopaedics and Related Research®
A Publication of The Association of Bone and Joint Surgeons®

Basic Research

External Beam Irradiation Preferentially Inhibits the Endochondral Pathway of Fracture Healing: A Rat Model

Yongren Wu PhD, E. Lex Hanna MD, Robert E. Holmes MD, Zilan Lin MD, Alexander M. Chiaramonti MD, Russell A. Reeves MD, Daniel G. McDonald MS, Kenneth N. Vanek PhD, William R. Barfield PhD, Hai Yao PhD, Vincent D. Pellegrini Jr MD

Received: 20 December 2017 / Accepted: 13 June 2018 / Published online: 20 July 2018

Abstract

Background External beam irradiation is an accepted treatment for skeletal malignancies. Radiation acts on both cancerous and normal cells and, depending on the balance of these effects, may promote or impair bone healing after pathologic fracture. Previous studies suggest an adverse effect of radiation on endochondral ossification, but the existence of differential effects of radiation on the two distinct bone healing pathways is unknown.

Questions/purposes The purpose of this study was to investigate the differential effects of external beam irradiation on endochondral compared with intramembranous ossification with intramedullary nail and plate fixation of fractures inducing the two respective osseous healing pathways through assessment of (1) bone biology by histomorphometric analysis of cartilage area and micro-CT volumetric assessment of the calcified callus; and (2) mechanical properties of the healing fracture by four-point bending failure analysis of bending stiffness and strength.

Methods Thirty-six male Sprague-Dawley rats underwent bilateral iatrogenic femur fracture: one side was repaired with an intramedullary nail and the other with compression plating. Three days postoperatively, half (n = 18) received 8-Gray external beam irradiation to each fracture. Rodents were euthanized at 1, 2, and 4 weeks postoperatively (n = 3/group) for quantitative histomorphometry of cartilage area and micro-CT assessment of callus volume. The remaining rodents were euthanized at 3 months (n = 9/group) and subjected to four-point bending tests to assess stiffness and maximum strength.

Results Nailed femurs that were irradiated exhibited a reduction in cartilage area at both 2 weeks (1.08 ± 1.13 mm^2 versus 37.32 ± 19.88 mm^2; 95% confidence interval [CI] of the difference, 4.32-68.16 mm^2; p = 0.034) and 4 weeks (4.60 ± 3.97 mm^2 versus 39.10 ± 16.28 mm^2; 95% CI of the difference, 7.64-61.36 mm^2; p = 0.023)

This work was funded by the Department of Defense (VDP; contract W81XWH-13-1-0430), during the conduct of this study. One of the authors (VDP) received other funding from J and J/DePuy Orthopaedics (Warsaw, IN, USA), outside the submitted work. One of the authors (YW) received grants from the Department of Defense, during the conduct of this study.
Clinical Orthopaedics and Related Research® neither advocates nor endorses the use of any treatment, drug, or device. Readers are encouraged to always seek additional information, including FDA approval status, of any drug or device before clinical use.
Each author certifies that his or her institution approved the animal protocol for this investigation and that all investigations were conducted in conformity with ethical principles of research.
This work was performed at the Department of Orthopaedics and Physical Medicine, Medical University of South Carolina, Charleston, SC, USA.

Y. Wu, E. L. Hanna, R. E. Holmes, Z. Lin, A. M. Chiaramonti, R. A. Reeves, W. R. Barfield, H. Yao, V. D. Pellegrini, Department of Orthopaedics, Medical University of South Carolina, Charleston, SC, USA

D. G. McDonald, K. N. Vanek, Department of Radiation Oncology, Medical University of South Carolina, Charleston, SC, USA

Y. Wu, H. Yao, V. D. Pellegrini, Department of Bioengineering, Clemson-MUSC Bioengineering Program, Clemson University, Charleston, SC, USA

V. D. Pellegrini Jr (✉), John A. Siegling Professor and Chair, Department of Orthopaedics and Physical Medicine, MUSC, 96 Jonathan Lucas Street, CSB 708, MSC 622, Charleston, SC 29425, USA, email: pellegvd@musc.edu

All ICMJE Conflict of Interest Forms for authors and *Clinical Orthopaedics and Related Research*® editors and board members are on file with the publication and can be viewed on request.

Wolters Kluwer

compared with nonirradiated fractures. There was also a decrease in the volume ratio of calcified callus at 4 weeks (0.35 ± 0.08 versus 0.51 ± 0.05; 95% CI of the difference, 0.01-0.31; p = 0.042) compared with nonirradiated fractures. By contrast, there was no difference in cartilage area or calcified callus between irradiated and nonirradiated plated femurs. The stiffness (128.84 ± 76.60 N/mm versus 26.99 ± 26.07 N/mm; 95% CI of the difference, 44.67-159.03 N/mm; p = 0.012) and maximum strength (41.44 ± 22.06 N versus 23.75 ± 11.00 N; 95% CI of the difference, 0.27-35.11 N; p = 0.047) of irradiated plated femurs was greater than the irradiated nailed femurs. However, for nonirradiated femurs, the maximum strength of nailed fractures (36.05 ± 17.34 N versus 15.63 ± 5.19 N; 95% CI of the difference, 3.96-36.88 N; p = 0.022) was greater than plated fractures, and there was no difference in stiffness between the nailed and plated fractures.

Conclusions In this model, external beam irradiation was found to preferentially inhibit endochondral over intramembranous ossification with the greatest impairment in healing of radiated fractures repaired with intramedullary nails compared with those fixed with plates. Future work with larger sample sizes might focus on further elucidating the observed differences in mechanical properties.

Clinical Relevance This work suggests that there may be a rationale for compression plating rather than intramedullary nailing of long bone fractures in select circumstances where bony union is desirable, adjunctive radiation treatment is required, and bone stock is sufficient for plate and screw fixation.

Introduction

The skeleton is a common site of metastasis, more rarely primary malignancies, and the morbidity associated with bony involvement is substantial [1, 13, 14, 43]. Pain, pathologic fractures, and subsequent surgical procedures compromise patient quality of life and threaten independence and mobility [6, 12, 18, 39-41, 50]. External beam irradiation of destructive bony lesions is a widely accepted therapy to accomplish local disease control, prevent subsequent pathologic fracture, and facilitate healing of radiosensitive lesions that compromise skeletal structural integrity [7, 22, 28]. Radiation also potentially interferes with bone formation. In the immature skeleton, radiation inhibits chondrogenesis and physeal growth, whereas in the mature skeleton, there is a range of effects secondary to preferential damage to osteoblasts [8, 13, 33, 48]. Williams and Davies [48] state that radiation affects not only chondrogenesis, but also resorption of calcified cartilage and bone. Paradoxically, low radiation (0.5 Gy) has been found to promote osteoblast proliferation and fracture healing [11]. Radiation acts on both cancerous and healthy bone cells [38, 44] and may promote or impair bone healing after pathologic fracture fixation. Such are the poorly understood and competing effects of radiation on bone healing [42].

Casting and intramedullary nail fixation allow micromotion at the fracture site and result in healing primarily through endochondral ossification, whereas rigid fixation as achieved with compression plating results in healing primarily by intramembranous ossification [6, 12, 17, 19, 31]. Bonarigo and Rubin [7] suggested that cartilage callus formation in endochondral ossification is inhibited by radiation; they observed nonunion rates of 70% in irradiated pathologic fractures in patients treated with intramedullary fixation or casting [7]. In mouse [23] and rat [9, 11, 30, 36, 47] models, radiation limits callus formation, delays healing, and reduces biomechanical strength in both unfixed and nailed femur fractures. Collectively, these reports suggest an adverse effect of radiation on fracture healing through endochondral ossification. Other studies [9, 45, 47] demonstrated radiation had a minimal effect on intramembranous ossification in plated mandibular reconstruction, but we are aware of no data about intramembranous healing of long bones [21, 26]. Clinically, a strategy that matches fracture fixation with the specific local biologic environment rarely guides surgical treatment [32]. Pathologic fractures are typically treated with intramedullary nails based on their load-sharing properties, ability to bypass large adjacent segments of diseased bone, reduced surgical trauma, and ease of use [1, 2, 5, 15]. However, in select patients, in whom direct visualization of the fracture is necessary and adjacent segment bone loss is minimal, compression plate fixation may be a viable option. We propose that improved understanding of radiation effects on osseous healing may identify plate fixation as the preferred treatment for some fractures that require adjunctive radiation.

We hypothesize that external beam irradiation will preferentially impair fracture healing by endochondral compared with intramembranous ossification secondary to radiation-mediated inhibition of mineralization of the cartilage callus during its transition to bone. Accordingly, we anticipate that irradiated fractures treated with intramedullary nails will fail to ossify the cartilage callus, have a greater delay in healing, result in a greater number of radiographic nonunions, and have less mechanical strength than either nonirradiated nailed fractures or radiated fractures treated by plate fixation. Conversely, healing of irradiated fractures with rigid plate and screw fixation will be less impaired than radiated fractures treated with intramedullary nails; they will heal faster and have greater mechanical strength than those treated with intramedullary nails.

Our purpose was to investigate the differential effects of external beam irradiation on endochondral compared with intramembranous ossification with intramedullary nail and

plate fixation of fractures representing the two respective osseous healing pathways through (1) assessment of effects on bone biology by histomorphometric analysis of cartilage area and micro-CT volumetric assessment of the calcified callus; and (2) assessment of effects on the mechanical properties of the healing fracture by four-point bending failure analysis of bending stiffness and strength.

Materials and Methods

This study protocol was approved by our Institutional Animal Care and Use Committee (protocol number 3217) and the Animal Care and Use Review Organization of the Department of Defense. The Sprague-Dawley rat was utilized in this study because of its robust ability to achieve bony healing in vivo and biologic similarities to humans. Size constraints of smaller species such as mice preclude study of the two different fracture healing pathways because of the inability to achieve stable fracture fixation with both intramedullary nailing and compression plating.

Two cohorts (each n = 18) of skeletally mature 5-month-old male Sprague-Dawley rats (Harlan Laboratories Inc, Indianapolis, IN, USA) underwent controlled bilateral femur fracture and fixation with rigid compression plating of one femur and a custom dynamically locked intramedullary nail on the contralateral side (Fig. 1 A-B). Preoperatively, animals were randomly assigned to one of two treatment groups (radiation versus control) as well as predetermined euthanasia time points for either histomorphometry and micro-CT or mechanical testing.

Animals were singly housed in a helicobacter-free facility with ¼-inch corn cob bedding, except for the 2 weeks after surgery when animals were housed with cellulose-based bedding (Alfa-Dri®; Lab Supply, Fort Worth, TX, USA). Animals received 12-hour light/dark cycles and were housed in ventilated racks with an automatic watering system. They were allowed to eat ad libitum throughout the experiment and were given standard rodent chow (Teklad 2918; Envigo, Somerset, NJ, USA). Before all surgeries, animals were given 1.0 mg/kg buprenorphine-SR LAB (Zoopharm, Windsor, CO, USA) for 72 hours of analgesia as well as a single 10-mg/kg dose of enrofloxacin for infection prophylaxis. Animals were monitored twice daily for signs of pain for the first week after surgery and daily thereafter. If animals demonstrated excessive pain postoperatively, additional analgesics were considered and veterinarian consultation was obtained. All animals were permitted full activity postoperatively. The experimental group received bilateral external beam irradiation on postoperative Day 3 at a dose of 8 Gy, which was determined to be biologically equivalent to that used to treat metastatic adenocarcinoma in humans [30, 47, 49]. Animals from each cohort were euthanized at 1, 2, or 4 weeks (n = 3 at each point) to evaluate biologic events

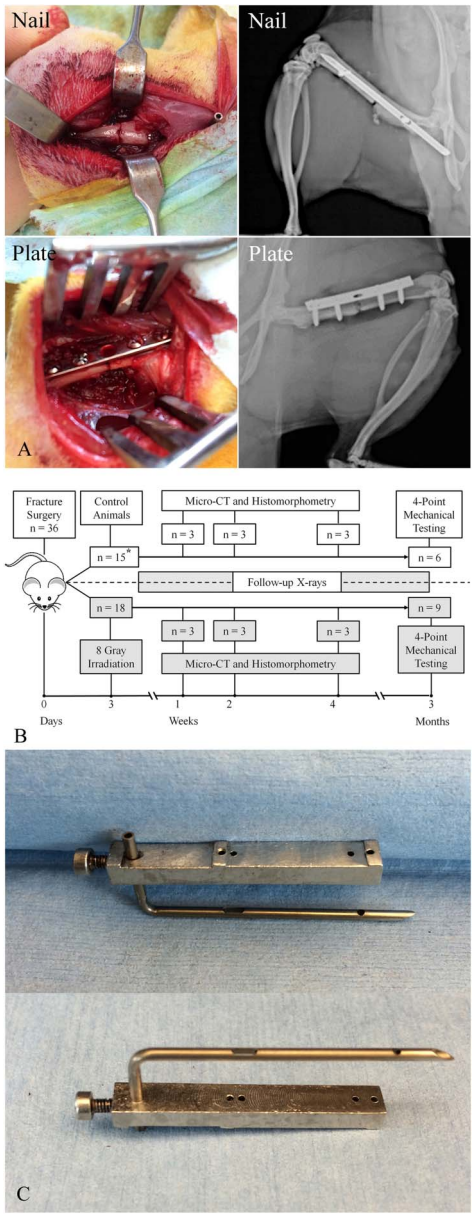

Fig. 1 A-C (**A**) A laterally based surgical approach to the femur was performed. Intraoperative photographs and postoperative radiographs demonstrate satisfactory fracture reduction with both intramedullary nailing and compression plating. (**B**) This diagram represents our overall experimental design. The timeline at the bottom of the figure represents the timing of irradiation and euthanasia for tissue analysis (micro-CT, histomorphometry, and mechanical testing). Both control and irradiated groups were subjected to scheduled radiographs throughout to monitor the progression of osseous healing and integrity of the fracture fixation. The asterisk denotes the discrepancy in the animal numbers as a result of three animals not completing the original schedule. (**C**) The intramedullary device was custom-designed as a dynamically locked intramedullary nail. It is made from a hollow metal needle with a locking screw insertion guide.

using histomorphometry and micro-CT and at 3 months (n = 9) to assess stiffness and strength of fracture healing using a four-point bending apparatus.

Bone Fracture and Fixation

A 3- to 4-cm skin incision was made on the lateral aspect of each thigh. For the compression plate, a power drill was used to create bicortical holes through the first and last holes of a 1.5-mm thick five-hole stainless steel plate prepositioned on the femur. Two 1.5 mm x 6-mm screws were placed eccentrically in these proximal and distal holes. A 0.76-mm smooth Kirschner wire on a power driver was then used to make at least three bicortical passes through the midshaft of the femur using the middle hole of the plate as a reference point. The plate was loosened, and a transverse fracture was created through the predrilled holes with a 6.35-mm osteotome and mallet. The fracture was reduced against the plate and the previously drilled eccentrically placed screws were tightened to compress the fracture. Additional fracture compression was achieved by sequentially placing screws in an eccentric fashion in the remaining two holes immediately adjacent to the fracture. Loosening the far screws, tightening the near screws, and then tightening the original far screws maximized compression across the fracture site and provided rigid fixation.

For the intramedullary nail, a transverse fracture was created at the midshaft using the same technique. A hand drill was introduced through the fracture into the medullary canal of the proximal fragment in a retrograde fashion, exiting proximally through the greater trochanter. Increasing size drill bits (1.3 mm, 1.5 mm, and 1.8 mm) were used sequentially in both fragments to enlarge the canal to accommodate the intramedullary device. A 0.8-mm Kirschner wire was inserted retrograde through the fracture site and out the greater trochanter, serving as a guidewire over which a custom dynamically locked intramedullary nail (Fig. 1 C) was inserted antegrade through the greater trochanter into proximal and then distal fragments. Using a custom drill guide, the distal locking screw was placed, the fracture was manually compressed, and the proximal locking screw was placed to rotationally secure the fracture around the nail. Serial radiographs were performed (Faxitron® LX-60, Tucson, AZ, USA) immediately postoperatively to assess fracture fixation as well as on postoperative Days 4, 10, 21, and 28 and in 2-week increments thereafter to monitor progression of osseous healing.

Radiation Exposure

On postoperative Day 3, the interventional group of animals underwent bilateral femoral radiation exposure using a 6.35-mm thick lead shield with a small aperture to restrict simultaneous x-ray exposure to both fracture sites. The PANTAK x-ray unit (Pantak Inc, East Haven, CT, USA) was operated at 250 kVp, 13 mA with 1.0 mm aluminum plus 0.5 mm copper-added filtration (half value layer 1.56 mm copper) to deliver a single dose of 8 Gy to each femur. For plated femora, the beam was directed parallel to the plate to minimize shielding and scatter. Prior analysis (Appendix, Supplemental Digital Content 1) determined that femora fixed by intramedullary nails received an effective radiation dose of 73.7%, whereas plated femora received an effective radiation dose between 61.4% and 80.0% of the nominally delivered dose depending on orientation of the plate to the radiation beam. Radiation doses used in treatment of malignant lesions in human bone approach 80 Gy compared with 8 Gy used for benign disease such as prophylaxis for heterotopic ossification after hip surgery. The 8 Gy in this study was determined to be biologically equivalent to human tumor dosing by virtue of the substantially smaller tissue mass in rats and is consistent with previous reports of fracture healing studies in rats and mice [30, 47, 49].

Outcome Measures

Thirty-five of the 36 animals survived the surgical procedure; one animal assigned to irradiation died as a result of intraoperative arterial bleeding. This animal was replaced with one initially designated as a control animal to ensure sufficient statistical power in our interventional radiation group. Two control animals were euthanized before the planned schedule, one secondary to postoperative hardware failure and the other from a toxic megacolon. All remaining animals were able to bear full weight on both hind limbs and ambulate without a visible limp immediately after surgery, and none had clinically apparent gait impairment leading up to the time of euthanasia.

To answer our first research question, assessing cartilage tissue area by histomorphometry and callus mineralization by micro-CT, we euthanized animals and harvested femora at 1, 2, and 4 weeks postoperatively and performed nondestructive micro-CT imaging of the fracture sites, acquiring images with 10-μm isotropic voxel size (70 kVp, 114 mA) using a Scanco μCT40 system (Scanco Medical, Wayne, PA, USA). Morphology and microstructure at the fracture site were assessed using a three-dimensional (3-D) volumetric reconstruction technique with measurements of the calcified callus volume (CV), femoral bone volume (BV), calcified callus volume ratio (CV/BV), calcified callus mineral density (CMD), femoral bone mineral density (BMD), and the corresponding bone mineral density ratios (CMD/BMD). Three sets of contours (the calcified callus

external to the bone, callus inside the femoral canal, and the original femur) were manually segmented on a series of micro-CT images using the tissue mineral density of the original femur bone (overall: 1180.57 mg HA/cm^3 ± 51.01 mg HA/ cm^3) as a reference. The volumes of calcified callus (aggregation of both external and internal callus) and original femur bone were calculated with a 3-D volumetric reconstruction technique using the Scanco μCT software. Internal and external callus was identified for each specimen by the same observer (YW); contiguous tissue that extended beyond the margin of the normal cortex proximal and distal to the fracture site was considered healing callus (Fig. 2 A-B).

Thereafter, we also performed quantitative histomorphometry on the same 1-, 2-, and 4-week specimens. En bloc femur specimens were fixed in 10% formalin, decalcified in 18% formic acid, and embedded in paraffin. The maximum midplane longitudinal cross-sections were collected, mounted on slides, and stained with either safranin O and fast green or hematoxylin and eosin. These two staining techniques provided clear differentiation among cartilage, fibrous tissue, and bone (Fig. 3 A-B).

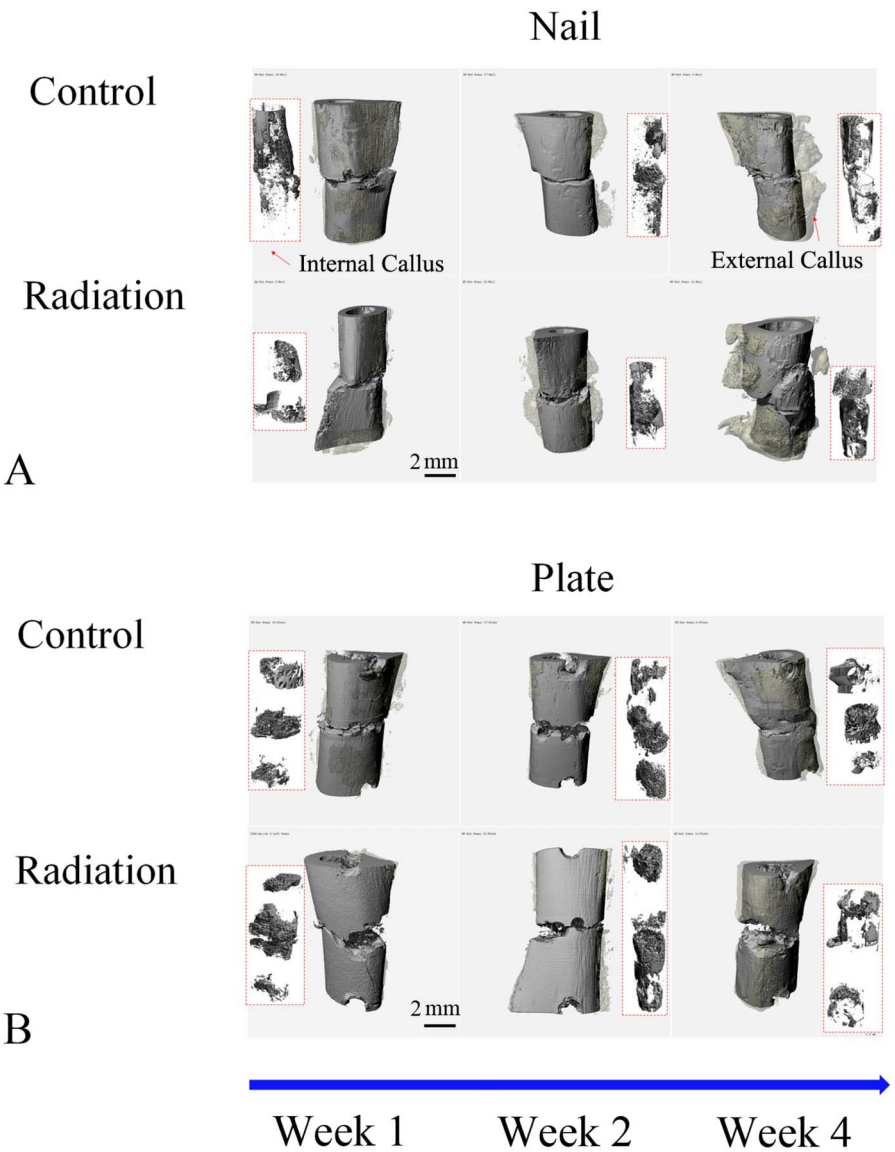

Fig. 2 A-B These images represent 3-D micro-CT reconstructions of the external and internal callus present around the fracture sites in rat femora using either nail (**A**) or rigid plate (**B**) fixation at Weeks 1, 2, and 4 postoperatively. The original femur and surrounding external callus are colored with solid and transparent gray, respectively. The internal callus is shown in the rectangle box inset (red outline).

Quantification of cartilage area at the fracture site was specifically assessed on the safranin O-stained histologic sections using a commercial histomorphometry software suite (Visiopharm, Broomfield, CO, USA). Paired side-to-side comparisons in each animal allowed for normalization of cartilage area and mitigated the variation implicit in comparisons between different animals.

To answer our second research question, assessing the stiffness and strength achieved through the two fracture healing pathways, we performed biomechanical testing on animals euthanized at 3 months using an electroforce testing system (BOSE; ELF3200, Minnetonka, MN, USA) with a four-point bending apparatus. The femora were stored in 0.9% (weight/volume) normal saline immediately on harvest to maintain normal tissue hydration. All internal fixation hardware was carefully removed to avoid disrupting the fracture and callus. Minimal bony overgrowth at 3 months was seen in both the plated and nailed specimens, resulting in little tissue disruption with hardware removal. Femora were immediately mounted with the femoral head pointing upward and the epicondylar axis directed vertically to simulate a physiologic varus loading moment (Fig. 4). The crosshead of the testing system was set at a fixed displacement rate of 0.01 mm/second and force was measured using a 225-N load cell. Specimens were subjected to increasing loading conditions until there was catastrophic failure or a clear indication that no additional force could be sustained. Two variables, stiffness and maximum strength, were measured. The slope of the linear region of the plotted force-displacement data was used to quantify bending stiffness. Maximum strength was defined as the point at which the measured force began to decrease despite increasing fracture displacement and was indicated by a decline in slope of the force-displacement curve [10, 14].

Statistical Analysis

For early progression of osseous healing, cartilage tissue area assessed by histomorphometry and femoral callus volume and mineral density assessed by micro-CT were examined to detect differences attributable to fixation method (plate versus nail), treatment group (radiation versus control), and postoperative time point (1, 2, and 4 weeks). We conducted data analysis using IBM SPSS Statistics, Version 24 (Armonk, NY, USA). Three-way analysis of variance (ANOVA) was used to test the interaction among fixation method, treatment group, and time. Two-way ANOVA was used to test the interaction between fixation method and time and between treatment group and time. At each time point, we used independent

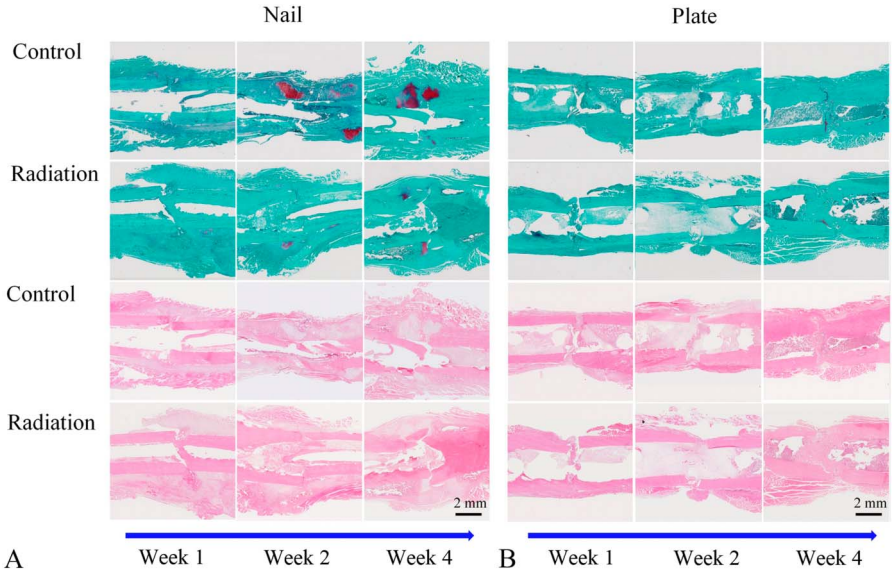

Fig. 3 A-B Assessment of the cartilage area surrounding the fracture site was performed using safranin-O staining and quantitative histomorphometry. Longitudinal cross-sections of fractures treated with either an intramedullary nail (**A**) or compression plate (**B**) are shown at postoperative Weeks 1, 2, and 4. Specimens were stained with safranin O and fast green in the upper panels or hematoxylin and eosin in the lower panels (original magnification, x 10). Photomicrographs were automatically stitched using Visiopharm histomorphometric software. In the upper panels (safranin-O/fast green), bright red areas around the fracture represent cartilage, whereas green areas represent fibrous tissue and bone.

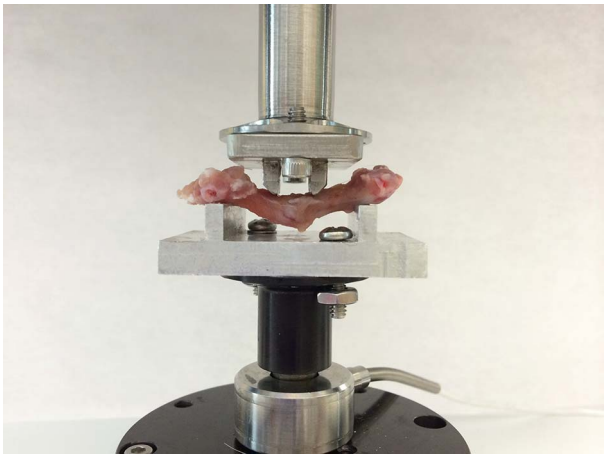

Fig. 4 Mechanical testing of femurs was performed through use of a four-point bending apparatus. The outer and inner spans of the four-point bending noses are 25 mm and 6.5 mm, respectively. The radius of each bending nose is 3 mm. Each femur specimen was placed in the testing apparatus to simulate a physiological varus loading condition with the femoral head directed upward, the transepicondylar axis oriented vertically, and the crosshead oriented to apply the designated load to the medial aspect of the femur.

t-tests to evaluate differences between irradiated and nonirradiated femora and between intramedullary nail and plate-fixed femora. We conducted three separate statistical analyses: (1) histomorphometric cartilage area to reflect changes in cartilage formation and maturation during fracture healing; (2) calcified callus volume ratios (CV/BV) from micro-CT reflecting changes in size of the calcified callus; and (3) calcified callus mineral density ratios (CMD/BMD) from micro-CT reflecting progression of callus mineralization.

For biomechanical testing at 3 months postoperatively, statistical analysis was carried out using paired comparisons between the two femora from the same animal to minimize the potentially large range of quantitative mechanical testing data obtained from different animals. A general linear mixed model was used to analyze the interaction between fixation method and radiation exposure. A random-effect term for each individual rat was included in the model to take advantage of the matched-pair design of the study. Analysis was completed using the 'lmer' function in the 'lme4' package in statistical programming software R version 3.3 (R Foundation, Vienna, Austria). Alpha was set at $p \leq 0.050$.

Additionally, effect size and power analyses (PASS 15 Sample Size, Kaysville, UT, USA) were performed at all points to determine the sample sizes necessary to demonstrate statistically significant differences with an α of 0.050, a desired power of at least 80%, and the difference between means and SDs based on previous data derived from similar experimental measurements with this model. Because we do not know the true population means and SDs, we based our effect size on prior observations of osseous healing in the nonirradiated bilateral fracture model in the rat (unpublished data), which demonstrated that biologic assays exhibit stable and narrow sample variability. Based on our data, we estimated a clinically meaningful difference among groups for micro-CT and histology at 20%; smaller differences in surrogates of fracture healing, although detectable using the described techniques, would not provide compelling evidence to influence clinical practice in favor of plate fixation given the ease of use and cumulative experience using intramedullary devices for fracture fixation, Accordingly, we estimated that effect sizes were between 0.60 and 0.80, indicating that the number of animals assigned to each group was sufficient to show statistically significant differences based on our cross-section within and among the group comparison models (Appendix, Supplemental Digital Content 2).

Results

Fracture healing progressed in all animals during the 3-month postoperative period, but radiation impaired callus formation and consolidation on serial plain radiographs more profoundly in fractures repaired by intramedullary nails than those repaired with plates and screws (Fig. 5).

The Effects of Radiation on the Biology of Fracture Healing at Weeks 1, 2, and 4

During the first 4 weeks after fracture, external beam irradiation exerted an inhibitory effect preferentially on endochondral ossification as exhibited in the nailed femurs. Radiation decreased cartilage area (Table 1) and calcified callus volume (CV/BV; Table 2) in the nailed femurs but had no effect in plated fractures. Specifically, in fractures fixed with nails that received radiation, there was a reduction in cartilage area at 2 weeks (1.08 ± 1.13 mm^2 versus 37.32 ± 19.88 mm^2; 95% confidence interval [CI] of the difference, 4.32-68.16 mm^2; $p = 0.034$) and 4 weeks postoperatively (4.60 ± 3.97 mm^2 versus 39.10 ± 16.28 mm^2; 95% CI of the difference, 7.64-61.36 mm^2; $p = 0.023$) compared with nonirradiated nailed fractures (Fig. 6). Similarly, nailed femurs that received radiation exhibited a decrease in the volume ratio of calcified callus (CV/BV) by micro-CT at 4 weeks (0.35 ± 0.08 versus 0.51 ± 0.05; 95% CI of the difference, 0.01-0.31; $p = 0.042$) compared with nonirradiated nailed fractures (Fig. 7). By contrast, there was no difference in cartilage area or calcified callus between radiated and nonradiated fractures

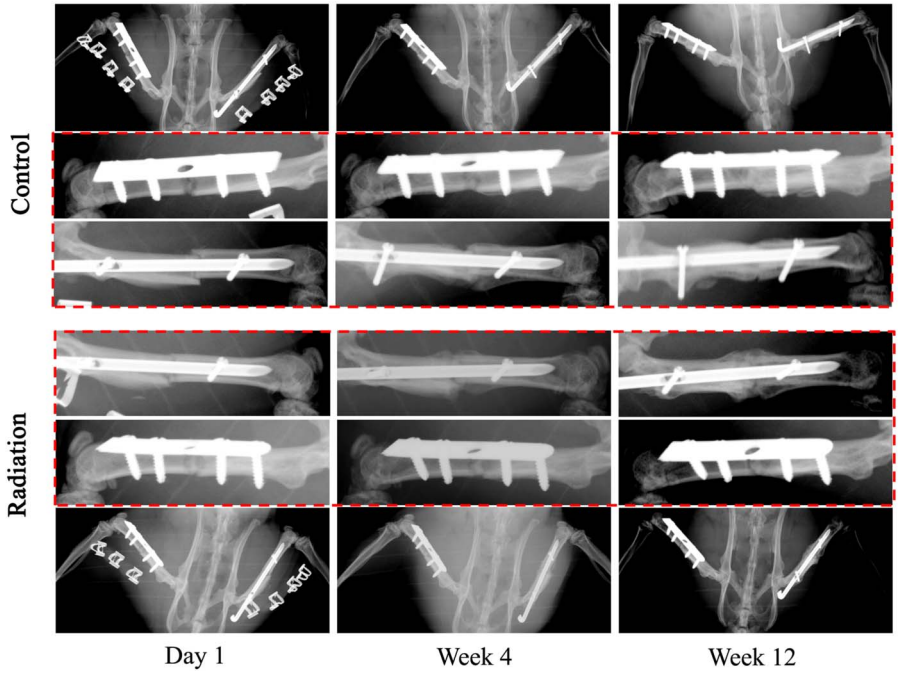

Fig. 5 Serial plain radiographs were obtained on all postoperative animals at regular prespecified intervals to assess for hardware integrity as well as progression to bony union of the fractures. Representative images are provided of a control and irradiated animal from postoperative Day 1 through postoperative Week 12.

repaired with plates. Radiation had no effect on calcified callus mineral density (CMD/BMD; Fig. 8) in either nailed or plated femora (Table 3).

As expected, in the absence of radiation exposure, fractures treated by intramedullary nails demonstrated a larger cartilage callus than those fixed with plates.

Table 1. Cartilage area

		Radiation (n = 9)		
Cartilage area (mm^2)	Control (n = 9) Mean ± SD	Mean ± SD	Mean difference versus control (95% confidence interval)	p value (radiation versus control)
Nail				
1 week	5.26 ± 3.33	0.05 ± 0.09	5.21 (-0.13 to 10.55)	0.092
2 weeks	37.32 ± 19.88	1.08 ± 1.13	36.24 (4.32-68.16)	**0.034**
4 weeks	39.10 ± 16.28	4.60 ± 3.97	34.5 (7.64-61.36)	**0.023**
Two-way ANOVA interaction: time versus radiation treatment				**0.048**
Plate				
1 week	3.74 ± 3.57	1.42 ± 1.17	2.32 (-3.70 to 8.34)	0.347
2 weeks	2.12 ± 2.37	1.67 ± 2.89	0.45 (-5.54 to 6.44)	0.840
4 weeks	2.48 ± 2.86	8.81 ± 8.80	6.33 (-8.50 to 21.16)	0.253
Two-way ANOVA interaction: time versus radiation treatment				0.273
Three-way ANOVA interaction: time, fixation methods, and radiation treatment				**0.026**

Histomorphometric analysis of safranin-O-stained tissue sections was performed to quantify the total cartilage area around the fracture sites; cartilage areas are expressed as means with SDs and compared between radiation and control animals with mean differences and 95% confidence intervals; differences between radiation and control are assessed by t-test; the effect of both time and treatment (radiation versus control) is assessed by two-way analysis of variance (ANOVA); the effect of time, fixation method (plate versus nail), and treatment (radiation versus control) is assessed through three-way ANOVA; the bold values represent significant differences at $p < 0.050$.

Table 2. CV/BV

CV/BV	Control (n = 9) Mean ± SD	Radiation (n = 9) Mean ± SD	Mean difference versus control (95% confidence interval)	p value (radiation versus control)
Nail				
1 week	0.07 ± 0.02	0.09 ± 0.02	0.02 (-0.03 to 0.07)	0.240
2 weeks	0.13 ± 0.05	0.15 ± 0.08	0.02 (-0.13 to 0.17)	0.840
4 weeks	0.51 ± 0.05	0.35 ± 0.08	0.16 (0.01-0.31)	**0.042**
Two-way ANOVA interaction: time versus radiation treatment				**0.035**
Plate				
1 week	0.10 ± 0.02	0.11 ± 0.02	0.01 (-0.04 to 0.06)	0.800
2 weeks	0.24 ± 0.06	0.16 ± 0.11	0.08 (-0.12 to 0.28)	0.362
4 weeks	0.30 ± 0.09	0.29 ± 0.08	0.01 (-0.18 to 0.20)	0.791
Two-way ANOVA interaction: time versus radiation treatment				0.635
Three-way ANOVA interaction: time, fixation methods, and radiation treatment				0.061

Micro-CT was used to quantify the volume of the calcified callus (CV) compared with the total volume of the femora bone (BV: 79.93 ± 7.84 mm^3); CV/BV ratios are expressed as means with SD, mean differences, and their 95% confidence intervals; treatment comparisons (radiation versus control) are assessed by t-tests; two-way interactions between time and treatment (radiation versus control) are compared with two-way analysis of variance (ANOVA); the three-way interaction of time, fixation method (plate versus nail), and treatment (radiation versus control) is assessed with a three-way ANOVA; the bold values represent significant differences at $p < 0.050$.

In nonradiated control fractures, those repaired with nails exhibited greater cartilage area at 2 (37.32 ± 19.88 mm^2 versus 2.12 ± 2.37 mm^2; p = 0.038) and 4 weeks (39.10 ± 16.28 mm^2 versus 2.48 ± 2.86 mm^2; p = 0.019) compared with those treated with plates.

The Effects of Radiation on the Biomechanical Strength of Fracture Healing at 3 Months

At 3 months after fracture repair, plated femurs demonstrated greater biomechanical strength as demonstrated by greater femoral stiffness and maximum strength compared

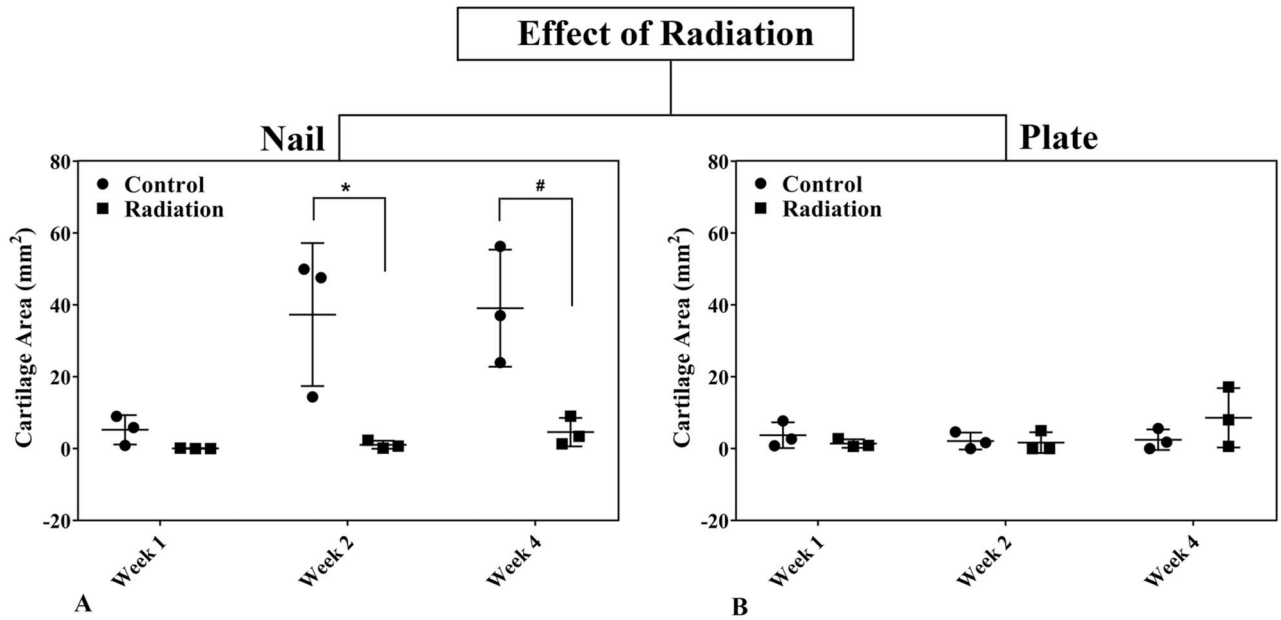

Fig. 6 A-B The effects of radiation on the cartilage area around fracture sites in rat femora using nail (**A**) or plate (**B**) fixation at postoperative Weeks 1, 2, and 4 are shown. Statistical significance (*) is portrayed with Student's t-test for paired comparisons at each time point. Error bars represent SD for the dot plot at each time point.

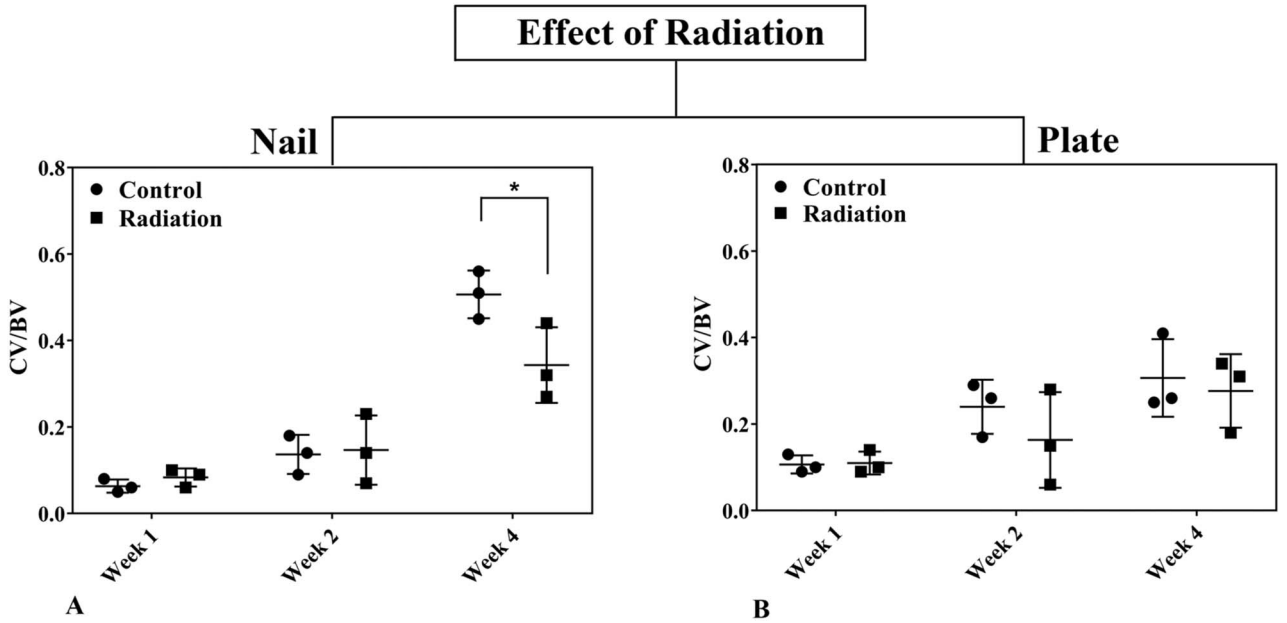

Fig. 7 A-B The effect of radiation on the fracture callus was assessed comparing the calcified callus volume ratio (CV/BV) in rat femora using nail (**A**) or plate (**B**) fixation at Weeks 1, 2, and 4 postoperatively. Statistical significance (*) is portrayed for ANOVA considering time, fixation method, and radiation as well as pairwise interactions. Student's t-test is portrayed for paired comparisons at each time point. Error bars represent SD for the dot plot at each time point.

with nailed femurs. An inhibitory effect of radiation on endochondral ossification was evident in both bending stiffness and maximum strength (Table 4); stiffness decreased by 48% and maximum force decreased by 34% in irradiated compared with nonirradiated fractures treated with nails. Uniquely, this impairment of fracture healing

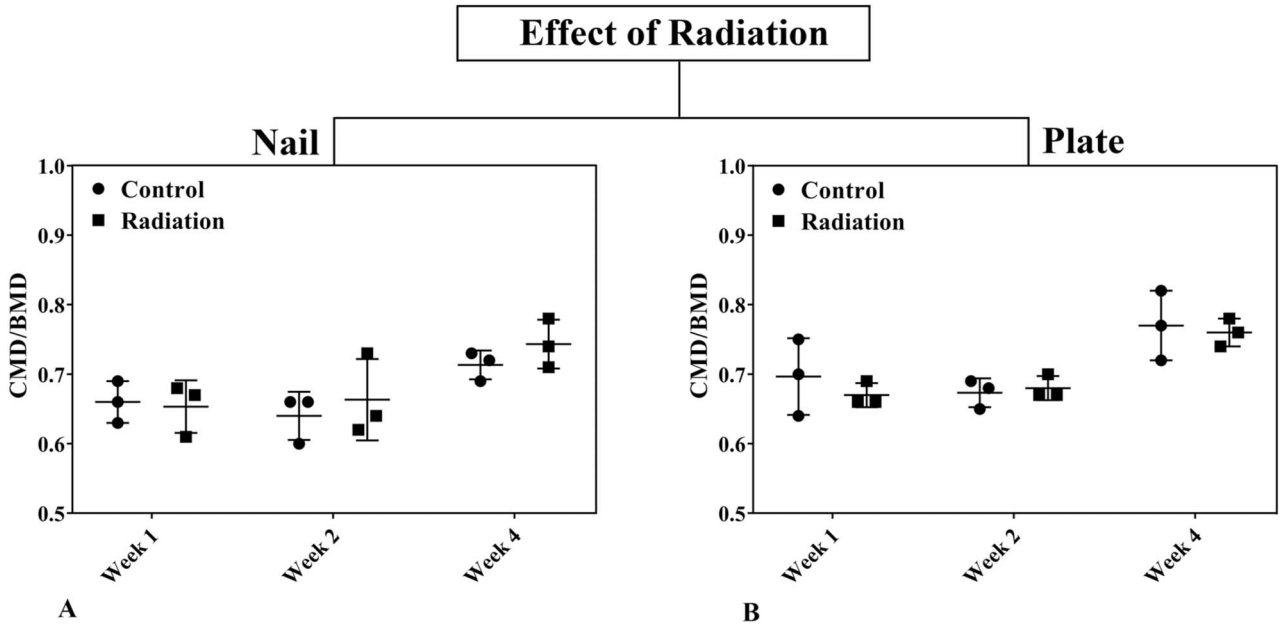

Fig. 8 A-B The effects of radiation on the calcified callus mineral density ratio (CMD/BMD) ratio in rat femora using nail (**A**) or plate (**B**) fixation at Weeks 1, 2, and 4 postoperatively are shown. Statistical significance (*) is portrayed for ANOVA considering time, fixation method, and radiation as well as pairwise interactions. Student's t-test is portrayed for paired comparisons at each point. Error bars represent SD for the dot plot at each time point.

Table 3. CMD/BMD

CMD/BMD	Control (n = 9) Mean ± SD	Radiation (n = 9) Mean ± SD	Mean difference versus control (95% confidence interval)	p value (radiation versus control)
Nail				
1 week	0.66 ± 0.03	0.66 ± 0.04	0 (-0.08 to 0.08)	0.957
2 weeks	0.64 ± 0.03	0.66 ± 0.06	0.02 (-0.09 to 0.13)	0.580
4 weeks	0.71 ± 0.02	0.74 ± 0.04	0.03 (-0.04 to 0.10)	0.371
Two-way ANOVA interaction: time versus radiation treatment				0.974
Plate				
1 week	0.70 ± 0.05	0.67 ± 0.02	0.03 (-0.06 to 0.12)	0.401
2 weeks	0.67 ± 0.02	0.68 ± 0.02	0.01 (-0.04 to 0.06)	0.612
4 weeks	0.77 ± 0.05	0.75 ± 0.02	0.02 (-0.07 to 0.11)	0.524
Two-way ANOVA interaction: time versus radiation treatment				0.573
Three-way ANOVA interaction: time, fixation methods, and radiation treatment				0.853

Micro-CT was performed to compare the callus mineral density (CMD) with the bone mineral density (BMD: 1180.57 ± 51.01 mg HA/cm^3); CMD/BMD ratios are expressed as means with SDs, the mean differences in radiated versus control femurs with their 95% confidence intervals; radiation versus control comparisons are made by t-tests; the interaction between time and treatment (radiation versus control) on CMD/BMD is assessed by a 2-way analysis of variance (ANOVA); the interaction among time, fixation method (plate versus nail), and treatment (radiation versus control) is assessed by three-way ANOVA.

biomechanics was preferentially evident with nailed femurs healing by endochondral ossification. Specifically, plated femurs that were irradiated exhibited nearly fivefold greater stiffness (128.84 ± 76.60 N/mm versus 26.99 ± 26.07 N/mm; 95% CI of the difference, 44.67-159.03 N/mm; p = 0.012) and nearly twice the maximum strength (41.44 ± 22.06 N versus 23.75 ± 11.00 N; 95% CI of the difference, 0.27-35.11 N; p = 0.047) compared with nailed femurs that were irradiated (Fig. 9).

In the control nonirradiated femurs, maximum strength of the nailed fractures (36.05 ± 17.34 N versus 15.63 ± 5.19 N; 95% CI of the difference, 3.96-36.88 N; p = 0.022) was 2.3 times greater than for the plated fractures. There was, however, no difference in stiffness between nailed (52.16 ± 46.75 N/mm versus 58.70 ± 18.77 N/mm; 95% CI of the difference, -39.29 to 52.37 N; p = 0.760) and plated fractures (Fig. 9).

Discussion

Treatment of pathologic fractures is complex, requiring consideration of characteristics unique to the patient, the

Table 4. Mechanical properties

Mechanical properties	Nail Mean ± SD	Plate Mean ± SD	Mean difference versus nail (95% confidence interval)	p value (plate versus nail)
Control (n = 6)				
Stiffness (N/mm)	52.16 ± 46.75	58.70 ± 18.77	6.54 (-39.29 to 52.37)	0.760
Maximum strength (N)	36.05 ± 17.34	15.63 ± 5.19	20.42 (3.96-36.88)	**0.022**
Radiation (n = 9)				
Stiffness (N/mm)	26.99 ± 26.07	128.84 ± 76.60	101.85 (44.67-159.03)	**0.012**
Maximum strength (N)	23.75 ± 11.00	41.44 ± 22.06	17.69 (0.27-35.11)	**0.047**
General linear mixed model interaction (fixation methods versus radiation treatment)				**0.010** (stiffness) **0.002** (maximum strength)

Femora were harvested at 3 months postoperatively and subjected to a four-point bending test; femoral stiffness and maximum strength are expressed as means with SDs; comparisons between fracture fixation method (plate versus nail) are made through mean differences with associated 95% confidence intervals; statistical comparisons between fixation method are made with t-tests; a general linear model was used to assess the interaction between fixation method (plate versus nail) with treatment (radiation versus control); the bold values represent significant differences at p < 0.050.

underlying malignancy, and fracture healing biology. Most often pathologic fractures are repaired with intramedullary devices and frequently require adjunctive radiation to achieve adequate local control of the tumor. Prior studies have evaluated the effects of radiation on endochondral ossification by quantifying the production of calcified callus as well as torsional mechanical strength [9, 30, 36, 47]; however, to our knowledge, none has explored the differential effects of radiation on the two healing pathways in long bone fractures. Development of this bilateral fracture model uniquely allows for direct comparison of the two distinct fracture-healing pathways in the same animal exposed to different environmental conditions. Previous animal models have used a unilateral femur fracture with simple intramedullary pin fixation [2, 4, 8-10, 14]; however, quadrupeds with such rotationally unstable fractures will effectively ambulate on three legs resulting in nonphysiological weightbearing through the injured limb. In contrast, stable fixation of bilateral femur fractures in this model has resulted in immediate quadrupedal weightbearing and affords a unique opportunity to concurrently study differential effects on both fracture healing pathways in the same animal. In this study, we found that irradiation preferentially inhibits endochondral ossification over intramembranous ossification, as demonstrated by a reduction in cartilage area and calcified callus volume as well as a decrease in acquisition of mechanical strength through endochondral but not intramembranous ossification. This work provides important information for the clinician treating pathologic fractures that require adjunctive radiation therapy by demonstrating the differential effect of radiation on fractures healing by endochondral as compared with primary membranous ossification.

There are some limitations to this work. Although individual sample sizes at 1, 2, and 4 weeks after fracture repair were relatively small (n = 3/group), we found modest to large effect sizes at both 2- and 4-week time points, consistent with the working hypothesis that radiation preferentially inhibits endochondral ossification. Some analyses failed to yield statistical differences, which we suspect were primarily the result of the early and short time intervals for healing after fracture at which differences in the two healing pathways may not be evident with effect sizes ranging from 0.1 to 0.29. A post hoc power analysis (Appendix Supplemental Digital Content 2) was performed to determine the minimum sample sizes necessary to demonstrate significant differences at all time points and suggested very large experimental animal numbers (ranging from n = 12 to n = 1376 animals per treatment group) to show differences between radiated and nonirradiated plated femurs within 1 month of fracture repair. Histomorphometric analysis provides only two-dimensional information through the maximum longitudinal tissue cross-section of fractures; as such, it is conceivable, albeit unlikely, to over- or underestimate cartilage tissue area because of the geometry of the callus and the orientation of the tissue section. Histologically, it can be difficult to differentiate fibrous tissue from bone; however, it was easy to identify and measure cartilage tissue using these techniques. Further studies are designed to elucidate the specific biologic effects of radiation on neovascularization through immunohistochemistry. Biomechanical testing analysis was limited to direct paired

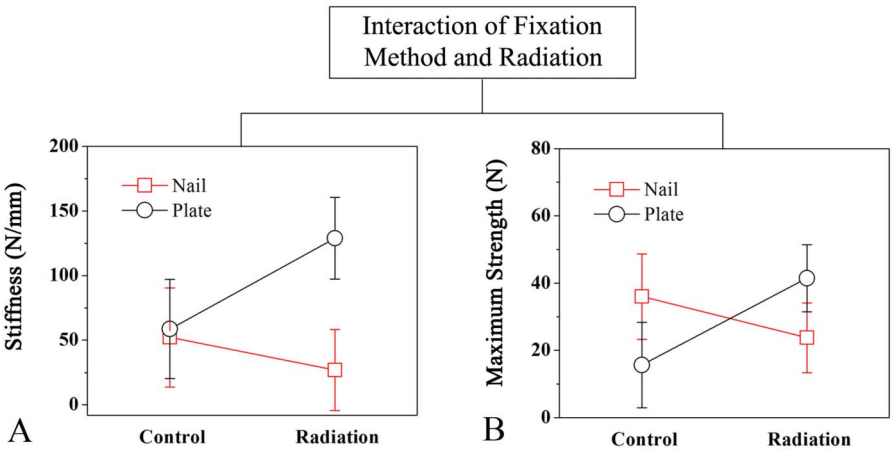

Fig. 9 A-B Four-point mechanical bending was performed on femurs harvested at 3 months postoperatively to measure stiffness and maximum strength. The interaction between fixation method (plate versus nail) and treatment (radiation versus control) on (**A**) stiffness and (**B**) maximum strength of the rat femur is shown. Multiple linear regression was used to assess the effects of radiation on nailed and plated femora. Error bars represent 95% CIs of the mean for each group.

comparison of plated versus nailed femurs in the same animals (control or irradiated) by primary study design. Future work might study the magnitude of radiation effects on fracture healing in the same animal (one limb irradiated, one limb shielded) with both femurs fixed using the same technique (bilateral nails or plates) followed for 6 months after fracture. Finally, it is important to emphasize that we did not use a metastatic tumor model as a result of the complexity and variability inherent in producing a natural pathologic fracture; rather, we devised a simplified model to first investigate the effects of radiation on normal fracture healing. It must be recognized that in human patients with complex metastatic bony lesions, adjacent segment bone loss can preclude adequate fracture fixation with plates. In most patients, therefore, intramedullary nailing will be the preferred fixation method for malignant pathologic fractures. Nevertheless, this work provides a framework for understanding the radiation biology of fracture healing and the advantages of plate fixation of fractures, when possible, that require adjunctive radiation therapy [2, 37].

To explore the differential effects of radiation on the biologic aspects of the two distinct fracture healing pathways, we first studied bony callus production. The calcified callus volume fraction (CV/BV), calcified tissue mineral density ratio (CMD/BMD), and cartilage area can be used as surrogates for cartilaginous callus formation. As expected, all three measures in nonirradiated animals increased over time concurrent with the progression of fracture healing. Nailed femurs that were exposed to radiation exhibited markedly decreased cartilage area (Fig. 6A) and decreased CV/BV ratios (Fig. 7A) compared with nonirradiated nailed femurs. In fact, radiation-mediated inhibition of callus formation was of such magnitude that the nailed femurs subjected to radiation demonstrated callus parameters of a similar magnitude as those observed in the plated femurs that healed by intramembranous ossification. Corroborating previous work, these findings are indicative of a profound inhibition of callus formation in the nailed fractures that were exposed to radiation [11, 16, 34] and are consistent with the notion that radiation imparts inhibition of endochondral ossification. The selective and preferential nature of this inhibition of endochondral ossification is illustrated by the unchanged biologic fracture healing parameters observed in the plated femurs of the same radiated animals that healed by intramembranous ossification. We speculate that radiation-mediated inhibition of endochondral ossification may be the result of inhibition of neovascularization and subsequent mineralization of the cartilaginous callus during its transition to bone during endochondral ossification [3, 20, 27].

To determine the impact of radiation on the mechanical properties of fracture healing through the two distinct pathways of ossification, we performed four-point bending tests on radiated femurs harvested 3 months after repair with either intramedullary nails or plates and screws. Fractures healing through endochondral ossification after intramedullary nail fixation exhibited reduced biomechanical properties compared with bones healing by intramembranous ossification after plate fixation. The observed differences in biomechanical characteristics between nailed and plated femurs in the two cohorts further support the preferential inhibition of cartilage callus formation by radiation as seen in the 2- and 4-week specimens treated with nail fixation. One prior study [30] found that irradiated rat femurs (9 Gy at 3 days postoperatively) fixed with a single longitudinal Kirschner wire exhibited delayed fracture healing and reduced torsional strength compared with nonirradiated femurs at 4 weeks after fracture repair. In contrast, fracture healing and strength acquisition in plated femurs in our model proceeded relatively unimpaired by radiation, presumably because intramembranous ossification does not rely heavily on cartilage callus formation as an intermediary to bony healing. This is in keeping with the observation that low doses (2 Gy) of irradiation have a negligible effect on osteoblast function [24, 29, 35]. Similarly, Jacobsson et al. [25] showed that radiation exposure had little impact on normal bony remodeling, which is consistent with our observations that radiation had no meaningful influence on the biologic and biomechanical parameters of fracture healing by intramembranous ossification. It is interesting to note that the stiffness of healing nonradiated fractures was not different between nailed and plated femurs despite an increased maximum strength in the nailed cohort. This increase in maximum strength may be explained by the large mass of callus providing resistance to a bending moment in the nailed femur, whereas stiffness may be more influenced by the intrinsic material differences of the various tissues formed during primary versus secondary fracture healing [46]. Intramembranous ossification is comprised primarily of bone, whereas endochondral ossification includes both bone and calcified cartilage callus. Bone formed with primary healing in the plated femurs likely undergoes only elastic deformation. In contrast, the heterogeneous tissues formed with secondary healing of the nailed femurs undergo a mixture of both elastic and plastic deformation of bone and cartilage, respectively, and exhibit larger maximum bending strength.

This work represents the establishment and application of a bilateral femur fracture model in the Sprague-Dawley rat that provides for immediate physiologic quadrupedal weightbearing and has demonstrated a differential and preferential inhibitory effect of radiation on endochondral ossification compared with intramembranous ossification in fracture healing. In contrast to prior studies, this model allows concurrent study of the two different fracture healing pathways in the same animal and controls for systemic

differences between animals. These findings suggest that rigid internal plate fixation may be the preferred method of fracture repair in select instances when there is an anticipated need for adjuvant radiation therapy or other conditions are present that selectively impair endochondral ossification, bone quality is sufficient to provide screw purchase, and durable bony healing of the fracture is desirable. Future animal studies in metastatic disease models are warranted to further explore these potential clinical implications.

Acknowledgments We thank Raymond Boaz III PhD, and Elizabeth H. Slate PhD, for their valuable assistance in statistical analysis.

References

1. Al Husaini H, Wheatley-Price P, Clemons M, Shepherd FA. Prevention and management of bone metastases in lung cancer: a review. *J Thorac Oncol.* 2009;4:251–259.
2. Arvinius C, Parra JL, Mateo LS, Maroto RG, Borrego AF, Stern LL. Benefits of early intramedullary nailing in femoral metastases. *Int Orthop.* 2014;38:129–132.
3. Bell EG, McAfee JG, Constable WC. Local radiation damage to bone and marrow demonstrated by radioisotopic imaging. *Radiology.* 1969;92:1083–1088.
4. Bhandari M, Shaughnessy S. A minimally invasive percutaneous technique of intramedullary nail insertion in an animal model of fracture healing. *Arch Orthop Trauma Surg.* 2001;121:591–593.
5. Bickels J, Dadia S, Lidar Z. Surgical management of metastatic bone disease. *J Bone Joint Surg Am.* 2009;91:1503–1516.
6. Body JJ. Increased fracture rate in women with breast cancer: a review of the hidden risk. *BMC Cancer.* 2011;11:384.
7. Bonarigo BC, Rubin P. Nonunion of pathologic fracture after radiation therapy. *Radiology.* 1967;88:889–898.
8. Bonnarens F, Einhorn TA. Production of a standard closed fracture in laboratory animal bone. *J Orthop Res.* 1984;2:97–101.
9. Brown RK, Pelker RR, Friedlaender GE, Peschel RE, Panjabi MM. Postfracture irradiation effects on the biomechanical and histologic parameters of fracture healing. *J Orthop Res.* 1991;9:876–882.
10. Browner BD, Jupiter JB, Krettek C, Anderson P. *Skeletal Trauma: Basic Science, Management, and Reconstruction*. Philadelphia, PA, USA: Elsevier/Saunders; 2015.
11. Chen M, Huang Q, Xu W, She C, Xie ZG, Mao YT, Dong QR, Ling M. Low-dose x-ray irradiation promotes osteoblast proliferation, differentiation and fracture healing. *PloS One.* 2014;9:e104016.
12. Coleman RE. Bisphosphonates: clinical experience. *Oncologist.* 2004;9(Suppl 4):14–27.
13. Coleman RE. Clinical features of metastatic bone disease and risk of skeletal morbidity. *Clin Cancer Res.* 2006;12:6243s-6249s.
14. De Marinis F, Eberhardt W, Harper PG, Sureda BM, Nackaerts K, Soerensen JB, Syrigos K, Tredaniel J. Bisphosphonate use in patients with lung cancer and bone metastases: recommendations of a European expert panel. *J Thorac Oncol.* 2009;4:1280–1288.
15. Dijkstra S, Stapert J, Boxma H, Wiggers T. Treatment of pathological fractures of the humeral shaft due to bone metastases: a comparison of intramedullary locking nail and plate osteosynthesis with adjunctive bone cement. *Eur J Surg Oncol.* 1996;22:621–626.
16. Donneys A, Ahsan S, Perosky JE, Deshpande SS, Tchanque-Fossuo CN, Levi B, Kozloff KM, Buchman SR. Deferoxamine restores callus size, mineralization, and mechanical strength in fracture healing after radiotherapy. *Plast Reconstr Surg.* 2013;131:711e-719e.
17. Einhorn TA. The cell and molecular biology of fracture healing. *Clin Orthop Relat Res.* 1998;355(Suppl):S7–21.
18. Gaillard S, Stearns V. Aromatase inhibitor-associated bone and musculoskeletal effects: new evidence defining etiology and strategies for management. *Breast Cancer Res.* 2011;13:205.
19. Giannoudis PV, Einhorn TA, Marsh D. Fracture healing: the diamond concept. *Injury.* 2007;38(Suppl 4):S3–6.
20. Grabham P, Sharma P. The effects of radiation on angiogenesis. *Vasc Cell.* 2013;5:19.
21. Gullane PJ. Primary mandibular reconstruction: analysis of 64 cases and evaluation of interface radiation dosimetry on bridging plates. *Laryngoscope.* 1991;101:1–24.
22. Harrington KD. Orthopedic surgical management of skeletal complications of malignancy. *Cancer.* 1997;80:1614–1627.
23. Hayashi S, Suit HD. Effect of fractionation of radiation dose on callus formation at site of fracture. *Radiology.* 1971;101:181–186.
24. He J, Qiu W, Zhang Z, Wang Z, Zhang X, He Y. Effects of irradiation on growth and differentiation-related gene expression in osteoblasts. *J Craniofac Surg.* 2011;22:1635–1640.
25. Jacobsson M, Albrektsson T, Turesson I. Dynamics of irradiation injury to bone tissue. A vital microscopic investigation. *Acta Radiol Oncol.* 1985;24:343–350.
26. Klotch DW, Ganey T, Greenburg H, Slater-Haase A. Effects of radiation therapy on reconstruction of mandibular defects with a titanium reconstruction plate. *Otolaryngol Head Neck Surg.* 1996;114:620–627.
27. Korpela E, Liu SK. Endothelial perturbations and therapeutic strategies in normal tissue radiation damage. *Radiat Oncol.* 2014;9:266.
28. Larsson S. Treatment of osteoporotic fractures. *Scand J Surg.* 2002;91:140–146.
29. Lau P, Baumstark-Khan C, Hellweg CE, Reitz G. X-irradiation-induced cell cycle delay and DNA double-strand breaks in the murine osteoblastic cell line OCT-1. *Radiat Environ Biophys.* 2010;49:271–280.
30. Markbreiter LA, Pelker RR, Friedlaender GE, Peschel R, Panjabi MM. The effect of radiation on the fracture repair process. A biomechanical evaluation of a closed fracture in a rat model. *J Orthop Res.* 1989;7:178–183.
31. McKibbin B. The biology of fracture healing in long bones. *J Bone Joint Surg Br.* 1978;60:150–162.
32. Miller BJ, Soni EE, Gibbs CP, Scarborough MT. Intramedullary nails for long bone metastases: why do they fail? *Orthopedics.* 2011;34. doi: 10.3928/01477447-20110228-12.
33. Mitchell MJ, Logan PM. Radiation-induced changes in bone. *Radiographics.* 1998;18:1125-1136; quiz 1242–1243.
34. Nicholls F, Janic K, Filomeno P, Willett T, Grynpas M, Ferguson P. Effects of radiation and surgery on healing of femoral fractures in a rat model. *J Orthop Res.* 2013;31:1323–1331.
35. Park SS, Kim KA, Lee SY, Lim SS, Jeon YM, Lee JC. X-ray radiation at low doses stimulates differentiation and mineralization of mouse calvarial osteoblasts. *BMB Rep.* 2012;45:571–576.
36. Pelker RR, Friedlaender GE, Panjabi MM, Kapp D, Doganis A. Radiation-induced alterations of fracture healing biomechanics. *J Orthop Res.* 1984;2:90–96.
37. Ruggieri P, Mavrogenis AF, Casadei R, Errani C, Angelini A, Calabro T, Pala E, Mercuri M. Protocol of surgical treatment of long bone pathological fractures. *Injury.* 2010;41:1161–1167.
38. Sakurai T, Sawada Y, Yoshimoto M, Kawai M, Miyakoshi J. Radiation-induced reduction of osteoblast differentiation in C2C12 cells. *J Radiat Res.* 2007;48:515–521.

39. Santen RJ. Clinical review: effect of endocrine therapies on bone in breast cancer patients. *J Clin Endocrinol Metab.* 2011;96: 308–319.
40. Sathiakumar N, Delzell E, Morrisey MA, Falkson C, Yong M, Chia V, Blackburn J, Arora T, Brill I, Kilgore ML. Mortality following bone metastasis and skeletal-related events among women with breast cancer: a population-based analysis of US Medicare beneficiaries, 1999-2006. *Breast Cancer Res Treat.* 2012;131:231–238.
41. Schrading S, Schild H, Kuhr M, Kuhl C. Effects of tamoxifen and aromatase inhibitors on breast tissue enhancement in dynamic contrast-enhanced breast MR imaging: a longitudinal intra-individual cohort study. *Radiology.* 2014;271:45–55.
42. Suva LJ, Griffin RJ. The irradiation of bone: old idea, new insight. *J Bone Miner Res.* 2012;27:747–748.
43. Suva LJ, Washam C, Nicholas RW, Griffin RJ. Bone metastasis: mechanisms and therapeutic opportunities. *Nat Rev Endocrinol.* 2011;7:208–218.
44. Szymczyk KH, Shapiro IM, Adams CS. Ionizing radiation sensitizes bone cells to apoptosis. *Bone.* 2004;34:148–156.
45. Vestergaard P, Rejnmark L, Mosekilde L. Effect of tamoxifen and aromatase inhibitors on the risk of fractures in women with breast cancer. *Calcif Tissue Int.* 2008;82:334–340.
46. Wehner T, Steiner M, Ignatius A, Claes L. Prediction of the time course of callus stiffness as a function of mechanical parameters in experimental rat fracture healing studies–a numerical study. *PloS One.* 2014;9:e115695.
47. Widmann RF, Pelker RR, Friedlaender GE, Panjabi MM, Peschel RE. Effects of prefracture irradiation on the biomechanical parameters of fracture healing. *J Orthop Res.* 1993; 11:422–428.
48. Williams HJ, Davies AM. The effect of x-rays on bone: a pictorial review. *Eur Radiol.* 2006;16:619–633.
49. Woodard HQ. The influence of x-rays on the healing of fractures. *Health Phys.* 1970;19:791–799.
50. Yong M, Jensen AO, Jacobsen JB, Norgaard M, Fryzek JP, Sorensen HT. Survival in breast cancer patients with bone metastases and skeletal-related events: a population-based cohort study in Denmark (1999-2007). *Breast Cancer Res Treat.* 2011; 129:495–503.